Pharmaceutical Research, Vol. 25, No. 3, March 2008 (© 2007)
DOI: 10.1007/s11095-007-9343-z

Research Paper

Genetically Engineered Block Copolymers: Influence of the Length and Structure of the Coiled-Coil Blocks on Hydrogel Self-Assembly

Chunyu Xu[1] and Jindřich Kopeček[1,2,3]

Received January 23, 2007; accepted May 11, 2007; published online August 23, 2007

Purpose. To explore the relationship between the structure of block polypeptides and their self-assembly into hydrogels. To investigate structural parameters that influence hydrogel formation and physical properties.
Methods. Three ABA triblock and two AB diblock coiled-coil containing polypeptides were designed and biologically synthesized. The triblock polypeptides had two terminal coiled-coil (A) domains and a central random coil (B) segment. The coiled-coil domains were different in their lengths, and tyrosine residues were incorporated at selected solvent-exposed positions in order to increase the overall hydrophobicity of the coiled-coil domains. The secondary structures of these polypeptides were characterized by circular dichroism and analytical ultracentrifugation. The formation of hydrogel structures was evaluated by microrheology and scanning electron microscopy.
Results. Hydrogels self-assembled from the triblock polypeptides, and had interconnected network microstructures. Hydrogel formation was reversible. Denaturation of coiled-coil domains by guanidine hydrochloride (GdnHCl) resulted in disassembly of the hydrogels. Removal of GdnHCl by dialysis caused coiled-coil refolding and hydrogel reassembly.
Conclusions. Protein ABA triblock polypeptides composed of a central random block flanked by two coiled-coil forming sequences self-assembled into hydrogels. Hydrogel formation and physical properties may be manipulated by choosing the structure and changing the length of the coiled-coil blocks. These self-assembling systems have a potential as *in-situ* forming depots for protein delivery.

KEY WORDS: coiled-coils; genetically engineered polymers; hydrogels; self-assembly.

INTRODUCTION

Hydrogels are 3-dimensional hydrophilic polymer networks. They can absorb a large amount of water and remain insoluble. Based on their composition, hydrogels can be categorized as synthetic polymer based hydrogels, bio-polymer based hydrogels, or hybrid hydrogel systems, which contain both synthetic and biomolecular moieties.

The development of drug delivery systems for the sustained release of peptides/proteins is an interesting yet challenging task. In-situ-forming synthetic hydrogel systems have been shown to have a great potential in peptide/protein delivery (1–3). Recently, biopolymer-based hydrogel systems have also been developed to be *in-situ* forming and may be used for peptide/protein delivery (4–6).

One common feature of different hydrogel systems is the presence of crosslinks, either chemical or physical. Coiled-coil protein folding domains have been used as physical crosslinks for protein-based hydrogels (7–12). These consist of two or more α-helices winding around each other to form a superhelix (13). The primary sequence of a left-handed coiled-coil is characterized by a repeating heptad unit, $(abcdefg)_n$, and a and d are usually hydrophobic residues, whereas e and g are often charged residues. The stability and specificity of the coiled-coil structure can be determined by these hydrophobic and electrostatic interactions. The distinctive feature of coiled coils is the specific spatial recognition, association, and dissociation of helices, making it an ideal model of protein biomaterials, where the higher order structure may be predicted based on the primary sequence.

ABA triblock polypeptide copolymers, where A is a coiled-coil forming block and B is a random block, self-assemble into hydrogels (14,15). We have shown previously that minor, but tailored, modifications of the structure of the coiled-coil block A lead to dramatic changes in its properties. In the sequence $(VSSLESK)_6$, we replaced V with K in the a position of the fourth heptad to destabilize the hydrophobic interactions in the core, and three additional K residues replaced S in the c position of the third, fourth, and fifth heptads to introduce an electrostatic repulsive force between c and g residues. These changes resulted in a substantial decrease of the melting temperature, a change in the concentration needed for self-assembly, and changes in the oligomerization state (15).

[1] Department of Pharmaceutics and Pharmaceutical Chemistry, University of Utah, 30 S. 2000 E. Rm. 201, Salt Lake City, Utah 84112, USA.
[2] Department of Bioengineering, University of Utah, Salt Lake City, Utah 84112, USA.
[3] To whom correspondence should be addressed. (e-mail: Jindrich.Kopecek@utah.edu)

Solvent-exposed tyrosine residues in proteins have been found to be important in protein folding and stability. Using a double-mutant strategy, the aromatic–aromatic interaction of a solvent-exposed Y/Y pair on the first α-helix of barnase, the small ribonuclease from *Bacillus amyloliquefaciens*, was found to contribute to the protein stability (16). A conserved tyrosine was found in the neck domain of fungal kinesins, which was able to assume a two-stranded coiled-coil conformation (17,18). This solvent-exposed tyrosine was responsible for inhibiting the catalytic activity. Solvent-exposed tyrosine residues were also found to be important in receptor–ligand interaction in the epidermal growth factor molecules (19), as well as the calcium-dependent membrane association of 15-lipoxygenase-1 (20).

This study is an attempt to explore the relationship between the structure of the polypeptides, their self-assembly into hydrogels, and to investigate the parameters influencing the formation and physical properties of hydrogels. In addition, an understanding of the processes controlling the self-assembly of these polypeptides could represent an avenue to explore their potential in the design of delivery systems for peptides/proteins. The fact that self-assembly occurs in an aqueous environment suggests their potential for the development of *in-situ*-forming protein delivery systems. It is hypothesized that the coiled-coil association provides the most important crosslinking force in the hydrogel system possessing polypeptides made up of two terminal coiled-coil domains and one central random segment. It is also hypothesized that the tyrosine residues in the coiled-coils may increase the overall hydrophobicity of the coiled-coils. This may enhance the association of the coiled-coils, and further facilitate hydrogel formation. Here, we report the design of three ABA-type triblock and two BA-type diblock recombinant polypeptides, where tyrosines were incorporated into A blocks (the coiled-coil domains) of different lengths, and the B block is a water-soluble polyelectrolyte segment $[(AG)_3PEG]_{10}$ (14). The self-assembly of these polypeptides into hydrogels was evaluated.

MATERIALS AND METHODS

Materials

Isopropyl β-thiogalactoside (IPTG) was from Sigma (St. Louis, MO, USA). Ni-NTA agarose resin was from Qiagen (Santa Clarita, CA, USA). Micro BCA protein assay reagent kit used for protein concentration measurement was from Pierce (Rockford, IL, USA).

Enzymes *Nhe*I, *Spe*I, *Hpa*I, *Eco*RI, and T4 DNA ligase were from New England Biolabs (Beverly, MA, USA). Platinum *Pfx* DNA polymerase, 10 mM dNTP mixture, and Zero Blunt® TOPO® PCR cloning kit were purchased from Invitrogen Life Technologies (Carlsbad, CA, USA).

Library efficiency *Escherichia coli* strain DH5α was obtained from Invitrogen Life Technologies. BL21(DE3)-pLysS was from Novagen (Madison, WI, USA).

Surfactant-free 1.0 μm yellow-green fluorescent amidine-modified polystyrene latex beads were from Interfacial Dynamics Corporation (Portland, OR, USA). CytosealTM 60 was from Richard-Allan Scientific (Kalamazoo, MI, USA).

Construction of Expression Vectors for the Protein Polymers

To construct the expression vectors for diblock polypeptides (BA_5 and BA_6, here, B stands for B block with the sequence of $[(AG)_3PEG]_{10}$, and $A_{4–6}$ stands for the coiled-coil domains with 4–6 heptad repeats; see Fig. 1 for structures), chemically synthesized oligonucleotides encoding blocks A_4, A_5 and A_6 with *Spe*I and *Eco*RI enzyme sites were first cloned into pCR-Blunt II-TOPO plasmid. They were then cleaved from the plasmid with *Spe*I and *Eco*RI enzymes, and ligated with the fragment from *Spe*I/*Eco*RI-digested pRSETB-polymer I expression vector (15), resulting in the expression vectors for BA_4, BA_5 and BA_6.

To construct the expression vectors for triblock polypeptides (A_4BA_4 and A_6BA_6), chemically synthesized oligonucleotide encoding blocks A_4 and A_6 with *Hpa*I and *Nhe*I enzyme sites were first cloned into pCR-Blunt II-TOPO plasmid. They were then cleaved from the plasmid with *Hpa*I and *Nhe*I enzymes, and ligated with the fragment from *Hpa*I/*Nhe*I-digested pRSETB-BA_4 and BA_6 expression vectors, resulting in the expression vectors for A_4BA_4 and A_6BA_6.

For the expression vector of triblock A_5BA_5, a pair of primers were designed, which included *Hpa*I and *Nhe*I enzyme sites, respectively. Using the previously obtained plasmid pCR-Blunt II-TOPO-A_5 as the template, where the A_5 encoding a gene had *Spe*I and *Eco*RI sites, the PCR reaction was set up and a new A_5 encoding gene with *Hpa*I and *Nhe*I sites was obtained. This PCR product was first digested with *Hpa*I and *Nhe*I, and then ligated with the fragment from *Hpa*I/*Nhe*I-digested pRSETB-BA_5 expression vector, resulting in the expression vectors for A_5BA_5.

The scheme for expression vector construction is shown in Fig. 2. The structures of all vectors were verified by direct DNA sequencing.

Expression and Purification of the Protein Polymers

Escherichia coli BL21(DE3)pLysS competent cells were transformed with the expression vectors separately. Cultures were grown at 37°C in 1.5 l of LB medium, containing 50 μg/ml

A_4BA_4:

MHHHHHHVNADP**(ISSLESK)-(IYYLEYK)$_2$-(ISSLESK)**-
ASYRDPMG[$(AG)_3PEG]_{10}$ARMPTSADP-**(ISSLESK)-(IYYLEYK)$_2$-(ISSLESK)**

A_5BA_5:

MHHHHHHVNADP**(ISSLESK)-(IYYLEYK)$_3$-(ISSLESK)**-
ASYRDPMG[$(AG)_3PEG]_{10}$ARMPTSADP-**(ISSLESK)-(IYYLEYK)$_3$-(ISSLESK)**

A_6BA_6:

MHHHHHHVNADP**(ISSLESK)$_2$-(IYYLEYK)$_3$-(ISSLESK)**-
ASYRDPMG[$(AG)_3PEG]_{10}$ARMPTSADP-**(ISSLESK)$_2$-(IYYLEYK)$_3$-(ISSLESK)**

BA_5:

MHHHHHHVNASYRDPMG[$(AG)_3PEG]_{10}$ARMPTSADP-**(ISSLESK)-(IYYLEYK)$_3$-(ISSLESK)**

BA_6:

MHHHHHHVNASYRDPMG[$(AG)_3PEG]_{10}$ARMPTSADP-**(ISSLESK)$_2$-(IYYLEYK)$_3$-(ISSLESK)**

Fig. 1. Amino acid sequences of triblock and diblock polypeptides. Single-letter abbreviations for amino acid residues were used. Coiled-coil forming sequences are shown in *boldface type*.

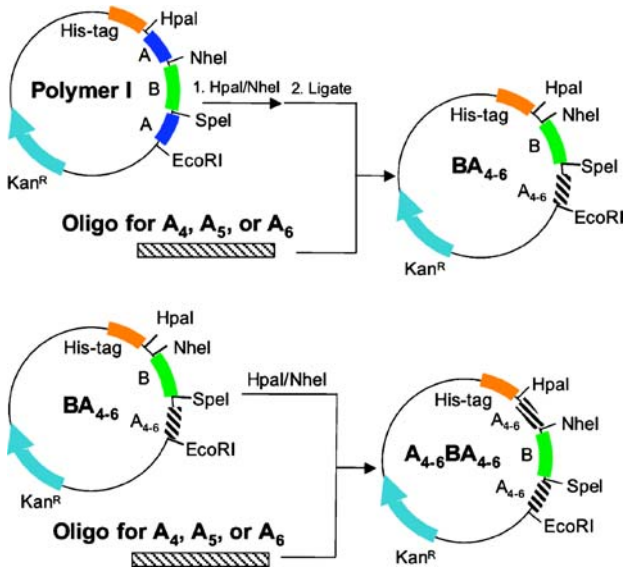

Fig. 2. Schematic presentation of the expression vector construction. **a** The construction strategy for diblock polypeptide expression vectors. **b** The construction strategy for triblock polypeptide expression vectors.

kanamycin and 34 μg/ml chloramphenicol, until their optical densities (OD_{600}) reached 1. Then, IPTG was added to a final concentration of 0.4 mM. Protein synthesis was induced at 37°C for 4 h before cells were harvested. The protein polymers were purified by immobilized metal affinity chromatography using Ni-NTA agarose resin (21). Bacterial cell pellets were first resuspended in Tris buffer (20 mM Tris, 500 mM NaCl, pH 6.9), and then sonicated and centrifuged at 15,000 rpm for 30 min at 4°C. The supernatants were loaded onto Ni-NTA columns pre-equilibrated with Tris buffer. The columns were washed sequentially with Tris buffer containing increasing concentrations of imidazole. The eluted fractions were analyzed by SDS-PAGE gel electrophoresis. The fractions containing the target protein polymers were loaded onto PD-10 columns containing Sephadex G-25, and eluted with 10 mM phosphate-buffered saline (PBS) buffer (10 mM phosphate, 150 mM NaCl, pH 7.4). The fractions were analyzed by SDS-PAGE, and the molecular weight and purity of the protein polymers were verified using matrix-assisted laser desorption/ionization time-of-flight mass spectrometry (MALDI-TOF MS).

Circular Dichroism Spectroscopy

An Aviv 62DS circular dichroism (CD) spectrometer with a thermoelectric temperature control system was used. The measurements were carried out at 25°C in 10 mM PBS buffer. The protein concentration used was 5 μM or 10 μM. Each sample was scanned from 200–250 nm at 1 nm per step. Three sequential scan data were averaged and subtracted from the buffer spectrum. For thermal stability experiments, the CD signal at 222 nm was recorded where the temperature was increased from 13°C to 94°C at 3°C per step. For each step, the sample was equilibrated for 1.5 min, followed by 30 sec of data point averaging. The thermal stability of each protein polymer at different pH was also evaluated. The transition temperatures were determined from the first-order differentiation of the CD signal at 222 nm with respect to temperature (22).

Analytical Ultracentrifugation

Sedimentation equilibrium experiments were performed on a Beckman Optima XL-A analytical ultracentrifuge, with an AnTi60 rotor, and six-channel, 12 mm thick, charcoal-epon centerpieces. All of the protein polymers were dissolved in 10 mM PBS buffer, and three different loading concentrations of 5, 25, and 50 μM were used. Samples were centrifuged to equilibrium with a rotor speed of 10,000 rpm at 20°C, and absorbance was recorded at 280 nm against a 10 mM PBS reference buffer. Equilibrium was confirmed by the overlays between scans taken at 4-h intervals. A baseline scan at a nonabsorbing wavelength (360 nm) was taken once the equilibrium was attained. Data were analyzed using nonlinear least squares techniques and NONLIN analysis program (23,24). The values of v-bar for each protein were calculated from the amino acid sequence (25).

Microrheology

Purified protein polymers were weighed and placed in plastic Eppendorf tubes. The appropriate amounts of deionized water and a suspension of 1.0 μm yellow-green fluorescent amidine-modified microspheres were added to each tube. The samples were mixed thoroughly and left for 10 days to permit the formation of hydrogels. Before the measurement, the samples were sealed between a microscope slide and a No. 1.5 glass cover slip with Cytoseal™ 60. The Brownian motion of the embedded particles at particular experimental conditions, including concentration, temperature, and pH, was observed with an epifluorescence optical microscope (Nikon Eclipse E800) using a 100×, NA=1.3, oil-immersion objective, and a CCD camera (Dage-MTI, DC330) with exposure times of 2 ms. To avoid wall effects, the focus plane was set at least 20 μm into the sample chambers. For each sample, 3,000 images were recorded using StreamPix software (Norpix Inc., Montreal, Canada) at intervals of 33 ms. Images were analyzed with IDL image analysis software (Research Systems Inc, Boulder, CO, USA) and the trajectories of the particles were extracted using algorithms developed and kindly provided by Crocker, Weitz and co-workers (26).

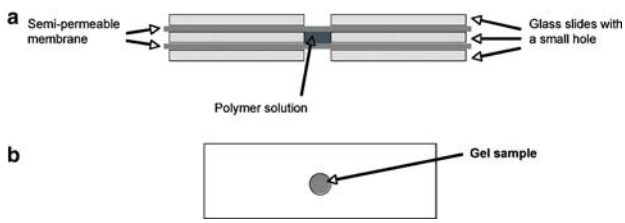

Fig. 3. Schematic diagram of the sandwich-like device. Polymer solution was loaded between the two semipermeable membranes. The device was immersed first in 100 mM GdnHCl, and then in distilled water. **a** Side view and **b** top view of the device.

Size Exclusion Chromatography

An ÄKTA fast performance liquid chromatography system, equipped with UV (280 nm) and differential refractometric detectors, was used for size exclusion chromatography. A Superdex peptide analytical column (Pharmacia, Uppsala, Sweden) was equilibrated with 10 mM PBS buffer or PBS buffer containing 30% acetonitrile at flow rate of 0.4 ml/min. The concentration used for the diblock polypeptides BA_5 and BA_6 was 1 mg/ml.

Scanning Electron Microscopy

The hydrogel samples were prepared similarly to the way they were prepared for microrheology experiments. The purified protein polymers were weighed and placed in Eppendorf tubes. A specific amount of deionized water was added and mixed with the polymers thoroughly. The samples were left at room temperature for 10 days to allow the formation of hydrogel. Next, additional aliquots of deionized water were added into the hydrogel samples and allowed to equilibrate for 3 more days. Then, the samples were shock-frozen in liquid nitrogen, and quickly transferred to a freeze-drier. The dried samples were then carefully fractured and their interior morphologies were examined using a scanning electron microscope (SEM) (Hitachi S-2460N SEM). Before SEM observation, the hydrogels were fixed on aluminum stubs and coated with gold for 40 s.

Unfolding/Refolding Study

A sandwich-like device was used in this study, as illustrated schematically in Fig. 3. Polypeptide solutions were first prepared at proper concentrations in distilled water, and then the solutions were loaded between the two semipermeable membranes. The device, containing the polypeptide solution, was then immersed in 1 M guanidine hydrochloride (GdnHCl) for 5 h, and then in distilled water for 3 days. After disassembly of the device, hydrogels were observed directly on the semipermeable membranes. They were then taken out, loaded on a glass slide, and observed with an optical microscope (Nikon Eclipse E800) using a 4× objective (NA=0.13) and a CCD camera (Dage-MTI, DC330).

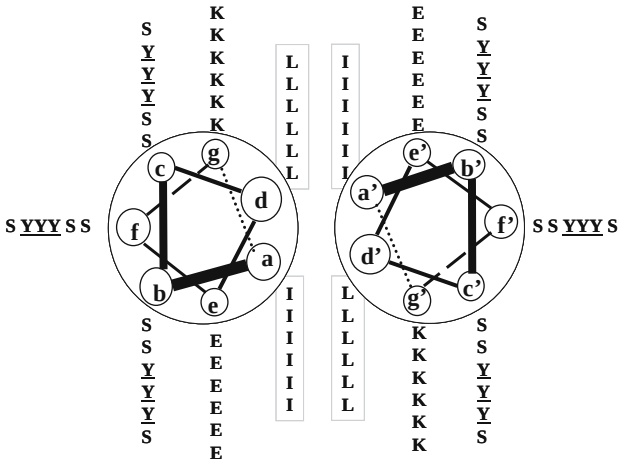

Fig. 4. Helical wheel diagram for A_6BA_6 triblock polypeptide. Tyrosine residues were *underlined*, and isoleucine and leucine were *boxed*.

Table I. Molecular Weights of Triblock and Diblock Polypeptides

Polypeptides	Calculated MW (Da)	Measured MW (Da)
A_4BA_4	16,822.30	16,794.04[a]
A_5BA_5	18,768.58	18,743.14[a]
A_6BA_6	20,258.27	20,258.00[b]
BA_5	14,076.19	14,057.78[a]
BA_6	14,821.03	14,820.40[b]

MW = molecular weight
[a] MALDI-TOF MS
[b] ESI-MS

RESULTS AND DISCUSSION

Amino Acid Sequences of the Protein Polymers

Three triblock (A_4BA_4, A_5BA_5, and A_6BA_6) and two diblock (BA_5 and BA_6) polypeptides were biologically synthesized. The amino acid sequences of these polypeptides are shown in Fig. 1, and a helical wheel diagram for A_6BA_6 is shown in Fig. 4. Block B is an AG-rich sequence $[(AG)_3PEG]_{10}$, which assumes a random coil structure and is water soluble (14). The coiled-coil domains A_4, A_5, and A_6 have 4 to 6 heptad repeats, and contain three tyrosine residues at the solvent-exposed positions b, c, and f in the 2nd and 3rd, 2nd, 3rd, and 4th, or 3rd, 4th, and 5th heptad units, respectively.

In order to evaluate the relationship between the structure of the triblock polypeptides and the physical properties of hydrogels based on these polypeptides, we varied the lengths of the A blocks—the coiled-coil domains, but kept the B block—the water-soluble segment unaltered. The reason for varying the A blocks is that we hypothesized that the association of the coiled-coil domains provided the physical crosslinking forces in the hydrogels. In our design, we chose I and L at a and d positions, which was intended to provide good hydrophobic packing at the interhelical core (27). In addition, we inserted tyrosine residues at the solvent-exposed positions in selected heptad repeats, which increased the overall hydrophobicity of the coiled-coils, and further enhanced the coiled-coil association. The two diblock polypeptides with 5 or 6 heptad repeats in the A blocks were designed in a similar manner, and were used to study the association of the coiled-coil domains.

Characterization of the Polypeptides

The molecular weights of the triblock and diblock polypeptides were determined by MALDI-TOF MS or ESI-MS (electrospray ionization MS). The experimental values agree with the theoretical calculations, as indicated in Table I.

Secondary structure was characterized by CD spectroscopy. All the triblock and diblock polypeptides showed predominant α-helical secondary structures, which were

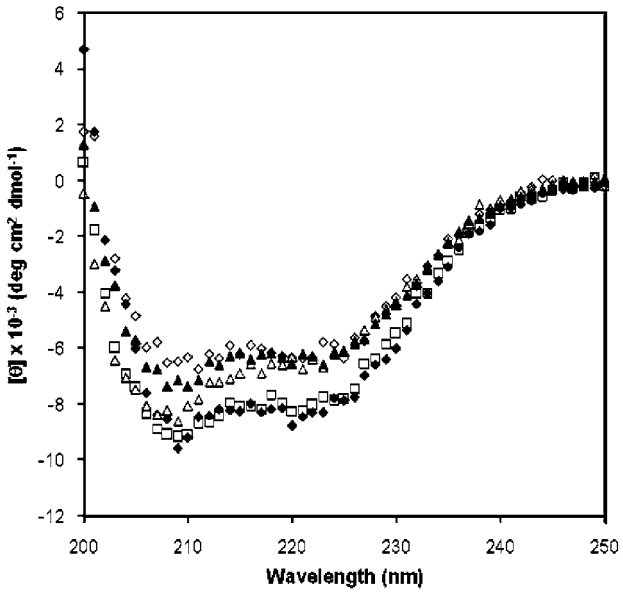

Fig. 5. CD spectra of 5 μM triblock and 10 μM diblock polypeptide solutions in PBS (pH 7.4) buffer at 25°C. *Open squares*, A_4BA_4; *open diamonds*, A_5BA_5; *filled diamonds*, A_6BA_6; *open triangles*, BA_5; *filled triangles*, BA_6.

indicated by the two characteristic negative peaks at 208 and 222 nm (Fig. 5).

Thermal responsiveness of the polypeptides was measured by monitoring the change of ellipticity at 222 nm with temperature (Fig. 6). The polypeptides with 5 or 6 heptad repeat units in their coiled-coil domains (A_5BA_5, A_6BA_6, BA_5, and BA_6) showed high degrees of thermal stability, indicated by a small change in the slopes of the melting

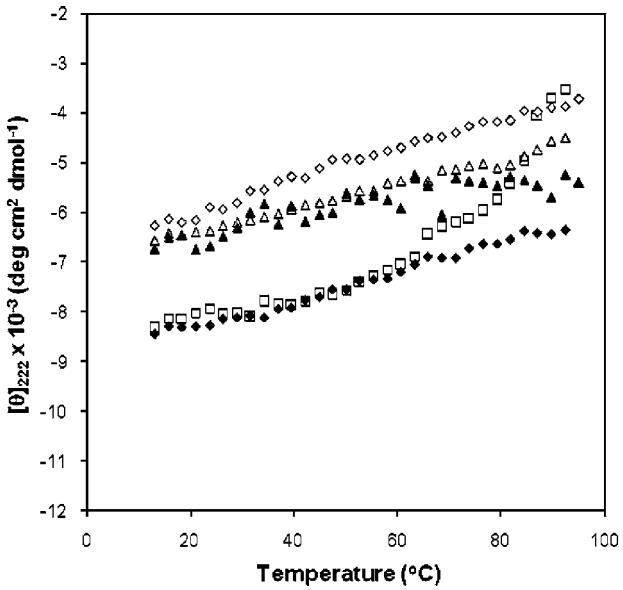

Fig. 6. Temperature dependence of the secondary structures of the triblock and diblock polypeptides. CD signal (molar ellipticity) at 222 nm as a function of temperature. *Open squares*, A_4BA_4; *open diamonds*, A_5BA_5; *filled diamonds*, A_6BA_6; *open triangles*, BA_5; *filled triangles*, BA_6.

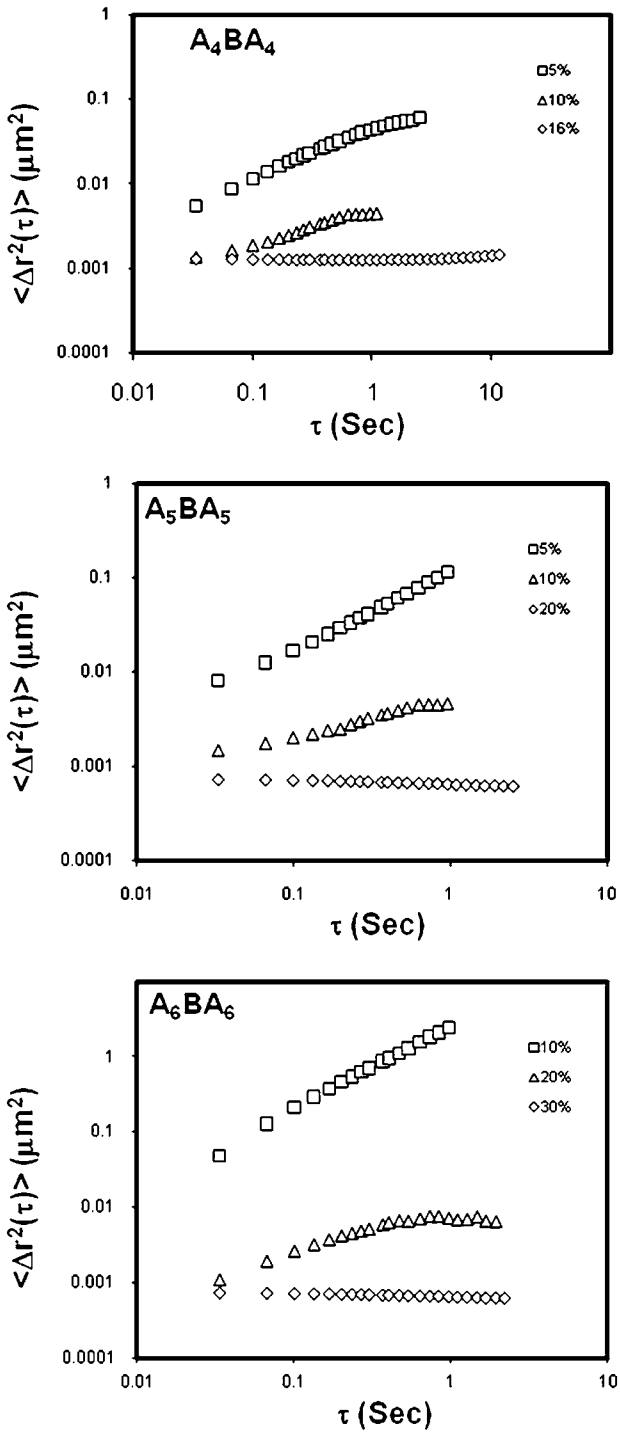

Fig. 7. Mean-square-displacement as a function of lag time for 0.5 μm amidine-modified spheres in triblock polypeptide water solutions. A_4BA_4, A_5BA_5, and A_6BA_6 are triblock polypeptides containing the coiled-coil domains, the A blocks, with 4, 5, and 6 heptad repeats, respectively.

curves. On the other hand, the polypeptide with 4 heptad repeats in the coiled-coil sequence (A_4BA_4) exhibited a transition in its melting curve around 85°C. The different thermal stabilities between A_4BA_4 and other polypeptides may be understood by their different structures. It is known

that hydrophobic interactions are the major stabilizing force in coiled-coils. The polypeptide A_4BA_4 has 4 heptad repeats in its coiled-coil blocks, while the other polypeptides (A_5BA_5, A_6BA_6, BA_5, and BA_6) have 5 or 6 heptads. As the chain length of the coiled-coil blocks increases, the number of hydrophobic interactions also increases (28). As a result, the polypeptide with shorter coiled-coil blocks A_4BA_4 is less stable than those with longer coiled-coil blocks (A_5BA_5, A_6BA_6, BA_5, and BA_6). However, the stability of the coiled-coils increases with the chain length nonlinearly (28). There is no significant difference between the coiled-coil blocks with 5 or 6 heptad repeats, resulting in a similar thermal stability among the polypeptides A_5BA_5, A_6BA_6, BA_5, and BA_6.

Hydrogel Formation from Triblock Polypeptides

Microrheology was used to evaluate the gelation behavior of the triblock polypeptides (A_4BA_4, A_5BA_5, and A_6BA_6). Using videomicroscopy (29) and multiple-particle-tracking technique (30,31), the time- and ensemble-averaged mean-square displacement (MSD) of the tracer particles as a function of time, $<\Delta r^2(\tau)>$, can be obtained from the particles' trajectories. When the particles are embedded in a viscous sample, they can diffuse freely and give a linear MSD-τ relationship with a slope of 1. If the particles are present in an elastic system, their movement will be largely constrained and the slope of MSD-τ curve will be 0 (30). The measurements from the triblock polypeptide water solutions indicated that A_4BA_4 formed hydrogel at the concentration of 16 wt.%, A_5BA_5 at 20 wt.%, and A_6BA_6 at 30 wt.% (Fig. 7). The inhomogeneous distribution of coiled-coil forming segments during self-assembly and the possibility of formation of intramolecular loops (32) are just two examples of processes that would result in an elastically ineffective association of helices. As A_6 blocks in A_6BA_6 possess the highest hydrophobicity, the dynamics of the rearrangement of network topology might be slower than that in polypeptides containing shorter A blocks.

Comparing the amino acid sequences of the triblock polypeptides (A_4BA_4, A_5BA_5, and A_6BA_6) used in this study with the polymer I from our previous study (15), where the B block was the same, and the coiled-coil block had the sequence of $(VSSLESK)_6$, there are two major differences. First, the a positions in the coiled-coil A blocks of the polypeptides A_4BA_4, A_5BA_5, and A_6BA_6 are all isoleucine residues, whereas those in the polymer I were valine residues. The other difference is that two or three heptad units in the A blocks of the polypeptides A_4BA_4, A_5BA_5, and A_6BA_6 have Y residues occupying the solvent-exposed b, c, and f positions, whereas those in the polymer I were all S residues. To evaluate the impact of hydrophobic interactions on the stability of coiled-coils, extensive investigations were focused on the effect of the amino acid substitution at a or d positions (33–36). The stability after a single substitution at position a in a model coiled-coil sequence was found to be directly correlated with the hydrophobicity of the substituted amino acid side chain (34). Since the triblock polypeptides A_4BA_4, A_5BA_5, and A_6BA_6 have 4 to 6 substitutions at positions a in each coiled-coil A block, the free energy change (ΔG) after the substitution at position a from V to I in these polypeptides could be greater or much greater than 0.8 kcal/mol, which is the value calculated from a single substitution at position a (34). The substitutions of S by Y at positions b, c, and f may lead to even larger free energy changes, although no thermodynamic data were reported for substitutions at these positions. As a result, the coiled-coil A blocks in the triblock polypeptides are quite stable, especially A_5BA_5 and A_6BA_6.

The analytical ultracentrifugation analysis of the two *diblock polypeptides* (BA_5 and BA_6) indicated that both fitted a trimer ⇔ hexamer equilibrium (data not shown), suggesting a strong association of the coiled-coil blocks. Furthermore, size exclusion chromatography of BA_5 and BA_6 at a concentration of 1 mg/ml showed a single peak in PBS, but two peaks in a mixed solvent (PBS+30% acetonitrile) (Fig. 8). This result suggests that both diblock copolymers, BA_5 and BA_6, form multimers in PBS; they partially dissociated when organic solvent was added.

However, the gelation concentrations of the polypeptide A_6BA_6 were higher than that of A_5BA_5 and A_4BA_4. The reason could be the formation of intramolecular loops, where the coiled-coil A blocks within the same triblock polypeptide molecule associate with each other (32). In order to form hydrogels, the coiled-coil A blocks have to interact intermolecularly. For the polypeptide A_6BA_6, the association of the coiled-coil blocks may have been too strong to break, and

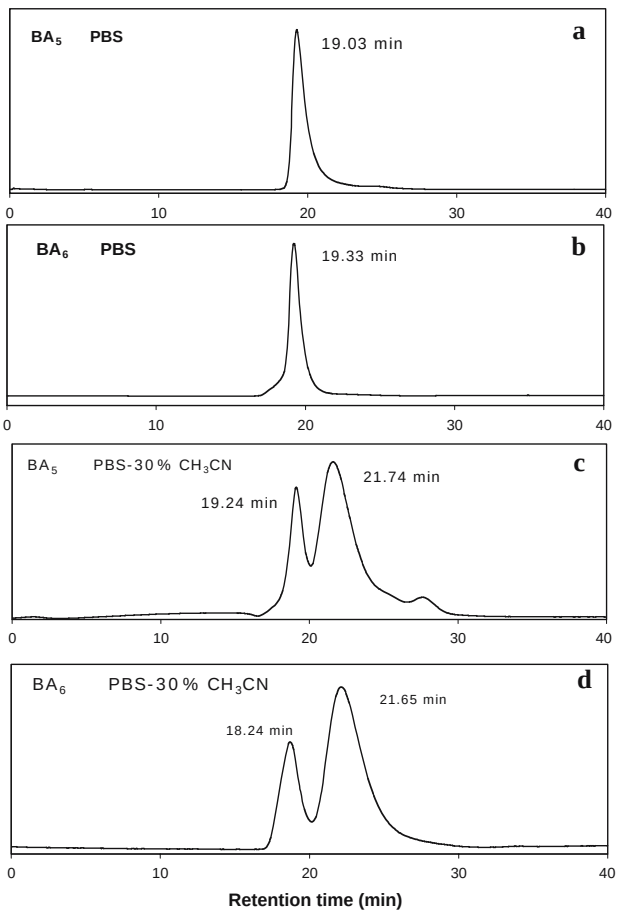

Fig. 8. Size exclusion chromatography of the diblock polypeptides BA_5 and BA_6 at 1 mg/ml. **a** BA_5 in PBS; **b** BA_6 in PBS; **c** BA_5 in PBS+30% acetonitrile; **d** BA_6 in PBS+30% acetonitrile.

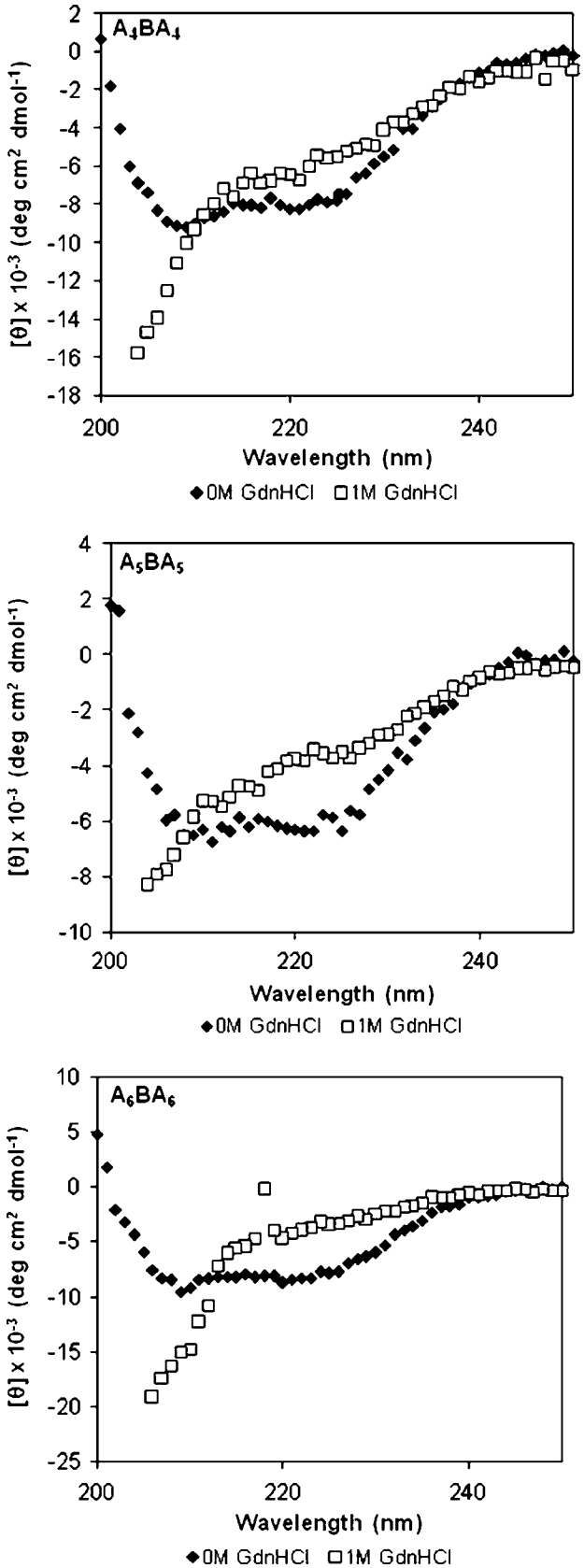

Fig. 9. Denaturation of the triblock polypeptides at 1 M GdnHCl.

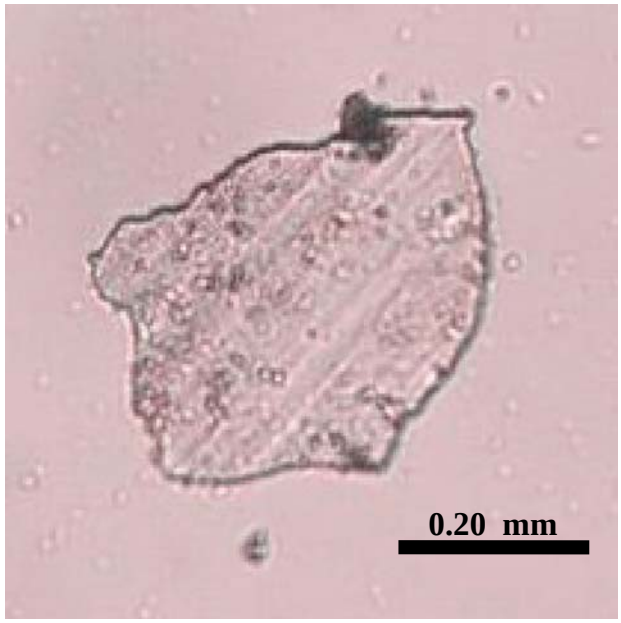

Fig. 10. A_4BA_4 sample (5 wt.%) after the unfolding/refolding process.

hence once the intramolecular loop formed, it would have been hard to re-establish the interaction and to form intermolecular associates. As a result, a higher concentration of polypeptide A_6BA_6 was required to form hydrogels, since the intramolecular loops do not contribute to the hydrogel formation.

Hydrogel Formation During Refolding of the A Blocks

In order to investigate whether the hydrogels will self-assemble following polypeptide denaturation, an unfolding/refolding study was carried out. CD spectra showed that the triblock polypeptides (A_4BA_4, A_5BA_5, and A_6BA_6) were denatured in 1 M GdnHCl (Fig. 9). Aqueous solutions

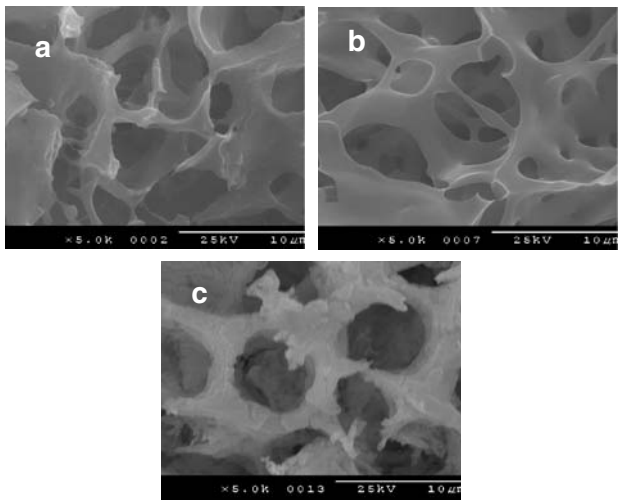

Fig. 11. SEM images of hydrogels self-assembled from triblock polypeptides. **a** 16 wt.% A_4BA_4; **b** 20 wt.% A_5BA_5; **C** 30 wt.% A_6BA_6.

of 5 wt.% A_4BA_4 and 20 wt.% A_6BA_6 were dialyzed against 1 M GdnHCl, then dialyzed against water as described in "Materials and Methods."

Hydrogels reformed in both 5 wt.% A_4BA_4 and 20 wt.% A_6BA_6 samples after unfolding/refolding process (Fig. 10). This result suggests that when the polypeptides were denatured and then allowed to refold slowly, hydrogels could be formed at lower concentrations, compared to the gelation concentration without the unfolding/refolding process (Fig. 7). This clearly suggests the importance of sample history on self-assembly of polypeptides. When in the denatured state, the macromolecules can thoroughly mix and the formation of coiled-coil crosslinks during refolding might be a statistically random process. Consequently, hydrogels with a more homogeneous distribution of crosslinks may form as a result. These are preliminary, but suggestive data; further detailed investigation of this phenomenon is warranted.

Morphology of the Hydrogels

To investigate the microstructure of the hydrogels, SEM was performed on three hydrogel samples: 16 wt.% A_4BA_4, 20 wt.% A_5BA_5, and 30 wt.% A_6BA_6. The samples were shock-frozen using liquid nitrogen followed by immediate lyophilization. All hydrogels showed interconnected network structures (Fig. 11), suggesting that hydrogels may be formed by physical crosslinking due to the association of coiled-coils. Our previous data demonstrated that in absence of hydrogel only a flat and tight texture was detectable after the same treatment (11), suggesting that the shock-frozen and quick-lyophilization process caused minimal effect on the samples.

CONCLUSIONS

In order to explore the relationship between the structure of triblock polypeptides containing coiled-coil domains and the physical properties of the hydrogels, and to investigate the parameters influencing the formation and physical properties of hydrogels, three ABA triblock and two AB diblock polypeptides were designed. The triblock polypeptides had two terminal coiled-coil domains and the same central random coil segment. The coiled-coil domains had different lengths, and tyrosine residues were incorporated at selected solvent-exposed positions to increase the hydrophobicity of the coiled-coil domains. The diblock polypeptides were used to study the association of the coiled-coil domains. Hydrogels self-assembled from solutions of triblock polypeptides, and had interconnected network microstructures. After the triblock polypeptides underwent a denaturation/refolding cycle, hydrogels were able to form at even lower concentrations. The results suggest that hydrogel self-assembly and their resulting physical properties may be influenced by other parameters, such as: the history of sample, length of the central random coil segment, formation of loops, and/or selective intermolecular association of the coiled-coil blocks. All these factors contribute to the molecular arrangement of polymer ingredients and are central to hydrogel performance (37). A thorough understanding of the relationship between the structure of block copolymers and the kinetics of their self-assembly is a prerequisite for the use of these materials in the development of *in-situ* forming hydrogels for the delivery of peptides and proteins.

ACKNOWLEDGEMENTS

We thank Drs. Bruce Yu and Jiyuan Yang for valuable discussions, Dr. David Tirrell for the kind gift of plasmid pUC18-RC, and Jon Callahan for critical reading of the manuscript. The research was supported in part by NIH grant EB005288.

REFERENCES

1. G. Tae, J. A. Kornfield, and J. A. Hubbell. Sustained release of human growth hormone from *in situ* forming hydrogels using self-assembly of fluoroalkyl-ended poly(ethylene glycol). *Biomaterials* **26**:5259–5266 (2005).
2. E. Ruel-Gariépy and J. C. Leroux. *In situ*-forming hydrogels—review of temperature-sensitive systems. *Eur. J. Pharm. Biopharm.* **58**:409–426 (2004).
3. E. Behravesh, K. Zygourakis, and A. G. Mikos. Adhesion and migration of marrow-derived osteoblasts on injectable *in situ* crosslinkable poly(propylene fumarate-co-ethylene glycol)-based hydrogels with a covalently linked RGDS peptide. *J. Biomed. Mater. Res. A* **65**:260–270 (2003).
4. B. Balakrishnan and A. Jayakrishnan. Self-cross-linking biopolymers as injectable *in situ* forming biodegradable scaffolds. *Biomaterials* **26**:3941–3951 (2005).
5. A. Motulsky, M. Lafleur, A. C. Couffin-Hoarau, D. Hoarau, F. Boury, J. P. Benoit, and J. C. Leroux. Characterization and biocompatibility of organogels based on L-alanine for parenteral drug delivery implants. *Biomaterials* **26**:6242–6253 (2005).
6. L. Zhang, E. M. Furst, and K. L. Kiick. Manipulation of hydrogel assembly and growth factor delivery *via* the use of peptide–polysaccharide interactions. *J. Control. Release* **114**:130–142 (2006).
7. C. Wang, R. J. Stewart, and J. Kopeček. Hybrid hydrogels self-assembled from synthetic polymers and coiled-coil domains. *Nature* **397**:417–420 (1999).
8. J. Kopeček, A. Tang, C. Wang, and R. J. Stewart. *De novo* design of biomedical polymers: Hybrids from synthetic macromolecules and genetically engineered protein domains. *Macromol. Symp.* **174**:31–42 (2001).
9. C. Wang, J. Kopeček, and R. J. Stewart. Hybrid hydrogels crosslinked by genetically engineered coiled-coil block proteins. *Biomacromolecules* **2**:912–920 (2001).
10. J. Yang, C. Xu, P. Kopečková, and J. Kopeček. Hybrid hydrogels self-assembled from HPMA copolymers containing peptide grafts. *Macromol. Biosci.* **6**:201–209 (2006).
11. J. Yang, C. Xu, C. Wang, and J. Kopeček. Refolding hydrogels self-assembled from N-(2-hydroxypropyl)methacrylamide graft copolymers by antiparallel coiled-coil formation. *Biomacromolecules* **7**:1187–1195 (2006).
12. C. Xu and J. Kopeček. Self-assembling hydrogels. *Polym. Bull.* **58**:53–63 (2007).
13. Y. B. Yu. Coiled-coils: stability, specificity, and drug delivery potential. *Adv. Drug Deliv. Rev.* **54**:1113–1129 (2002).
14. W. A. Petka, J. L. Harden, K. P. McGrath, D. Wirtz, and D. A. Tirrell. Reversible hydrogels from self-assembling artificial proteins. *Science* **281**:389–392 (1998).
15. C. Xu, V. Breedveld, and J. Kopeček. Reversible hydrogels from self-assembling genetically engineered protein block copolymers. *Biomacromolecules* **6**:1739–1749 (2005).
16. L. Serrano, M. Bycroft, and A. R. Fersht. Aromatic–aromatic interactions and protein stability. Investigation by double-mutant cycles. *J. Mol. Biol.* **218**:465–475 (1991).
17. F. Schafer, D. Deluca, U. Majdic, J. Kirchner, M. Schliwa, L. Moroder, and G. Woehlke. A conserved tyrosine in the neck

of a fungal kinesin regulates the catalytic motor core. *EMBO J.* **22**:450–458 (2003).
18. S. Adio, J. Reth, F. Bathe, and G. Woehlke. Review: regulation mechanisms of kinesin-1. *J. Muscle Res. Cell Motil.* **27**:153–160 (2006).
19. S. R. Campion, R. K. Matsunami, D. A. Engler, and S. K. Niyogi. Biochemical properties of site-directed mutants of human epidermal growth factor: importance of solvent-exposed hydrophobic residues of the amino-terminal domain in receptor binding. *Biochemistry* **29**:9988–9993 (1990).
20. M. Walther, R. Wiesner, and H. Kuhn. Investigations into calcium-dependent membrane association of 15-lipoxygenase-1. Mechanistic roles of surface-exposed hydrophobic amino acids and calcium. *J. Biol. Chem.* **279**:3717–3725 (2004).
21. E. Hochuli. Purification of recombinant proteins with metal chelate adsorbent. *Genet. Eng. (N Y)* **12**:87–98 (1990).
22. C. R. Cantor and P. R. Schimmel. *Biophysical Chemistry*, W. H. Freeman and Company, New York, 1980.
23. D. A. Yphantis. Eqilibrium ultracentrifugation of dilute solutions. *Biochemistry* **3**:297–317 (1964).
24. M. L. Johnson, J. J. Correia, D. A. Ypahantis, and H. R. Halvorson. Analysis of data from the analytical ultracentrifuge by non-linear least squares techniques. *Biophys. J.* **36**:575–588 (1981).
25. T. M. Laue, B. D. Shah, T. M. Ridgeway, and S. L. Pelletier. Computer aided interpretation of analytical sedimentation data for proteins. In S. E. Harding, A. J. Rowe, and J. C. Horton (eds.), *Ultracentrifugation in Biochemistry and Polymer Science*, The Royal Society of Chemistry, Cambridge, 1992, pp. 90–125.
26. J. C. Crocker, M. T. Valentine, E. R. Weeks, T. Gisler, P. D. Kaplan, A. G. Yodh, and D. A. Weitz. Two-point microrheology of inhomogeneous soft materials. *Phys. Rev. Lett.* **85**:888–891 (2000).
27. P. B. Harbury, T. Zhang, P. S. Kim, and T. Alber. A switch between two-, three-, and four-stranded coiled coils in GCN4 leucine zipper mutants. *Science* **262**:1401–1407 (1993).
28. J. Y. Su, R. S. Hodges, and C. M. Kay. Effect of chain length on the formation and stability of synthetic alpha-helical coiled coils. *Biochemistry* **33**:15501–15510 (1994).
29. J. C. Crocker and D. G. Grier. Methods of digital video microscopy for colloidal studies. *J. Colloid Interface Sci.* **179**:298–310 (1996).
30. T. G. Mason and D. A. Weitz. Optical measurements of frequency-dependent linear viscoelastic moduli of complex fluids. *Phys. Rev. Lett.* **74**:1250–1253 (1995).
31. F. C. MacKintosh and C. F. Schmidt. Microrheology. *Curr. Opin. Colloid Interface Sci.* **4**:300–307 (1999).
32. W. Shen, K. Zhang, J. A. Kornfield, and D. A. Tirrell. Tuning the erosion rate of artificial protein hydrogels through control of network topology. *Nat. Mater.* **5**:153–158 (2006).
33. K. Wagschal, B. Tripet, and R. S. Hodges. De novo design of a model peptide sequence to examine the effects of single amino acid substitutions in the hydrophobic core on both stability and oligomerization state of coiled-coils. *J. Mol. Biol.* **285**:785–803 (1999).
34. K. Wagschal, B. Tripet, P. Lavigne, C. Mant, and R. S. Hodges. The role of position a in determining the stability and oligomerization state of alpha-helical coiled-coils: 20 amino acid stability coefficients in the hydrophobic core of proteins. *Protein Sci.* **8**:2312–2329 (1999).
35. B. Tripet, K. Wagschal, P. Lavigne, C. Mant, and R. S. Hodges. Effects of side-chain characteristics on stability and oligomerization state of a *de novo*-designed model coiled-coil: 20 amino acid substitutions in position "d". *J. Mol. Biol.* **300**:377–402 (2000).
36. A. E. Keating, V. N. Malashkevich, B. Tidor, and P. S. Kim. Side-chain repacking calculations for predicting structures and stabilities of heterodimeric coiled coils. *Proc. Natl. Acad. Sci. U. S. A.* **98**:14825–14830 (2001).
37. J. Kopeček. Swell gels. *Nature* **417**:388–391 (2002).